Applied Catalysis B: Environmental 186 (2016) 184–192

Contents lists available at ScienceDirect

Applied Catalysis B: Environmental

journal homepage: www.elsevier.com/locate/apcatb

Photoelectrocatalytic degradation of the antibiotic sulfamethoxazole using TiO_2/Ti photoanode

Yuh-fan Su [a], Guan-Bo Wang [a], Dave Ta Fu Kuo [b,d,**], Meei-ling Chang [c], Yang-hsin Shih [a,*]

[a] Department of Agricultural Chemistry, National Taiwan University, Taipei 106, Taiwan
[b] Department of Architecture and Civil Engineering, City University of Hong Kong, Hong Kong
[c] Department of Environmental Engineering, Van Nung University, No.1, Van Nung Rd., Chung-Li, Tao-yuan 326, Taiwan
[d] City University of Hong Kong Shenzhen Research Institute, Shenzhen, China

ARTICLE INFO

Article history:
Received 27 August 2015
Received in revised form
23 December 2015
Accepted 4 January 2016
Available online 8 January 2016

Keywords:
Sulfamethoxazole (SMZ)
Titanium dioxide (TiO_2)
Photoelectrocatalytic
Chlorine
Radical scavengers

ABSTRACT

Photoelectrocatalysis (PEC) of sulfamethoxazole (SMZ) was investigated using TiO_2/Ti (UV-A) photoanode. Complete photoelectrocatalytic degradation of SMZ was achieved after 70 min at 0.5 V, while SMZ resisted to photolysis and electrolysis. Langmuir-Hinshelwood analysis yielded an adsorption constant (K) of 0.519 L/mg for the studied PEC-TiO_2 system, with K being 3–4 times of those from photocatalysis. PEC degradation of SMZ accelerated with increasing anodic potential (0–0.5 V), declining pH (from 10.1 to 2.7), and increasing NaCl concentration (1–100 mM). These trends were consistent with the understanding that higher potential gradient reduces recombination of holes and electrons, lower pH favors photoadsorption through modulation of SMZ speciation and TiO_2 surface charge, and higher Cl^- level encourages formation of chlorine radicals. Molar ratios of $HO^\bullet$ and chlorine radicals showed that the effects of pH and Cl^- levels were coupled, with the level of PEC activity linked to the relative dominance of [$Cl_2^{\bullet-}$] over [$HO^\bullet$]. In the presence of radical scavengers, SMZ photoelectrocatalysis was lowered by 30% at merely 10 mg/L of humic acid, and was reduced to <5% of the original rate at 10% methanol. The inhibitory effect of humic acid and methanol on PEC was consistent with the view that $HO^\bullet$ and $Cl_2^{\bullet-}$/active chlorine species were the main oxidants in a Cl^--present environment. A 3-times above-average photocurrent was observed in 10% methanol, whose unusual photocurrent increase was attributed to sequential current doubling – additional electron flow due to reactive adsorbate-hole interaction – through a series of proposed reactions: conversion of h^+_{VB}-bound methanol through formaldehyde and formic acid to CO_2. Implications of the findings with respect to practical application of PEC are presented.

1. Introduction

The occurrence of pharmaceuticals and their metabolites and transformation products in the environment is becoming a matter of concern because these compounds, which may have adverse effects on living organisms, are extensively and increasingly used in human and veterinary medicine and are released continuously into the environment [1]. Sulfamethoxazole (SMZ) is an important bacteriostatic agent that is commonly used in human and veterinary medicine [2]. The release of SMZ into the ecosystem or wastewater effluents has caused pollution and many human diseases [3]. Most antibiotics tested to date are known to be biorecalcitrant under aerobic conditions [4], thus escaping intact from conventional wastewater treatment plants. As a consequence, an intense research activity has been developed to find out efficient technologies aimed at removing these hazardous compounds from water.

Photocatalytic oxidation is one of the advanced technologies employed for the elimination of gaseous and aqueous organic pollutants because of the efficiency in their mineralization and ideally producing final products as carbon dioxide, water, and inorganic ions [5]. Widely used semiconductor photocatalyst, TiO_2, shows excellent UV-light photocatalytic activity and has been investigated extensively. The photocatalytic degradation of SMZ in water solutions during their illumination of UV radiation with TiO_2 catalyst was examined [1,6–12]. Abellan et al. [13,14] and Bayarri et al. [15] investigated the effect of TiO_2 concentration and light wavelength on the degradation kinetics of SMZ under simulated solar conditions, while Baran et al. [3] compared the efficiency of UV-A/TiO_2, UV-A/Fe^{3+} and UV-A/TiO_2/Fe^{3+} systems for the degradation of five sulfa drugs including SMZ. In their studies, several intermediates accompanying SMZ photocatalytic degradation and proposed respective reaction pathways were identified [2,13,16].

* Corresponding author.
** Corresponding author.
E-mail addresses: tfdkuo@cityu.edu.hk (D.T.F. Kuo), yhs@ntu.edu.tw (Y.-h. Shih).

http://dx.doi.org/10.1016/j.apcatb.2016.01.003
0926-3373/

Table 1
Experimental conditions for photoelectrocatalysis of SMZ, phenol, and BPA at 25 °C.

Group	C_0 (mg/L)	pH	NaCl (mM)	Anodic Potential (V)	Other Organic Compounds	Figure number in this study
SMZ						
I	13	5.4	10	1 (electrolysis)0.5 (PEC)	–	Fig. 2
II	2.4	5.4	10	0, 0.25, 0.5	–	Fig. 3
III	2.4	2.7, 5.4, 10.1	10	0.5	–	Fig. 4
IV	0.7, 1.3, 2.4, 13	5.4	10	0.5	–	Fig. 5
V	2.4	5.4	1, 10, 100	0.5	–	Fig. 6
VI	2.4	5.4	10	0.5	10 mg/L SRHA, 10% methanol	Fig. 7
phenol and BPA						
VII	2.4	5.4	10	0.5	–	Fig. 8

However, the catalyst is employed as slurry of fine particles in a photochemical reactor, which need to be separated at the end of the treatment in most photocatalytic applications [10]. In this work, TiO_2 film was immobilized on a Ti plate. The removal of SMZ was performed by photoelectrocatalytic degradation using TiO_2/Ti under UV-A irradiation. Photoelectrocatalysis (PEC) shows an advantage over photocatalysis since it applies a potential across a photoanode on which the catalyst is supported. This configuration allows for a more effective separation of the charges generated (e^-/h^+) in the process, thereby increasing the lifetime of the electron-hole pairs [17]. PEC has been shown to be effective in degrading small organic compounds [18–20], oilfield wastewater [21], and pharmaceuticals [22,23].

The objective of this study is to examine critical operational parameters that influence the photoelectrocatalytic degradation of antimicrobial agents. The effects of applied anodic voltage, initial pH, compound loading, electrolyte concentration, and presence of radical scavengers on PEC were investigated. As an antimicrobial compound commonly present in effluents of wastewater treatment plants, SMZ was used as the main test compound and two phenolic compounds, phenol and bisphenol A (BPA), one emerging contaminant, were also used in this study.

2. Materials and methods

All chemicals were reagent grade and used as received without further purification. SMZ was purchased from MP Biomedicals. Phenol and bisphenol A were both purchased from Acros Organics. The TiO_2/Ti electrode was prepared by treating a Ti foil in a solution containing 0.25% $TiCl_4$ and 16 M nitric acid at 65 °C for 1 h. The newly prepared TiO_2/Ti electrode was rinsed with DI water and then calcinated at 550 °C for 1.5 h. The TiO_2/Ti electrode was partially sealed with Teflon tape to define a geometrical area of 4 cm^2 for photoelectrocatalytic degradation of SMZ.

Basic characterization of the prepared TiO_2/Ti photoanode was performed. Field emission scanning electron microscopy (FE-SEM, JSM-7600F, JEOL) was used for imaging the surface morphology of the synthesized photoanode. The crystalline structures of TiO_2 nanorods were analyzed and determined by X-ray diffraction (XRD, BL 13A1, national synchrotron radiation research center (NSRRC), Taiwan). Specific surface area of the cleaned and air-dried TiO_2/Ti catalyst was determined by Brunauer-Emmett-Teller (BET) nitrogen adsorption at 77 K (Micromeritics ASAP 2010, USA).

The photoelectrocatalytic degradation of SMZ was conducted in a three-electrode cell irradiated by a 4 W UV-A Lamp combined with a potentiostat/galvanostat (614D, CHI). The cell was a 50 mL cylindrical glass vessel with Teflon cap. The cell was kept at 25 °C by using a cooling jacket and set at a distance of 1 cm from the irradiation lamp. The TiO_2/Ti electrode, the working electrode, was set such that only one side faced right at the lamp. The counter electrode was a Pt plate (1 × 1 cm^2) and the reference electrode was a $Ag/AgCl_{KCl(3\ M)}$ electrode. The supporting electrolyte was 10 mM NaCl solution except noted. Constant stirring was applied in all experiments via a Teflon stir bar. All experiments contained 40 mL of solution and the cell remained unsealed throughout the experiment.

At given intervals of irradiation, 5–15 μL of solution was withdrawn for SMZ analysis without further treatment or preparation. SMZ analysis was performed using an Agilent 1200 series HPLC equipped with a C_{18} column, a UV detector (at λ 267 nm), and a methanol/water (50/50 v/v) mobile phase at a flow rate of 0.6 mL min^{-1}. Photocurrent was measured using the potentiostat (614D CHI) as over the course of the reaction and time-averaged.

A total of seven groups of experiments were conducted: Group I compared the SMZ degradation by photoelectrocatalysis against that by photolysis and electrolysis; Group II examined the influence of anodic potential in the range of 0–0.5 V on SMZ photodegradation; Group III investigated the dependence of SMZ photoelectrocatalysis on initial solution pH, varying from 2.7 to 10.1; Group IV evaluated the dependence of degradation rate on initial SMZ concentrations and attempted to characterize the TiO_2 surface using Langmuir-Hinshelwood model; Group V examined the effect of NaCl concentration on SMZ photodegradation rate; Group VI tested the interference on SMZ degradation by in the presence of known radical scavengers, humic acid and methanol. Group VII examined the degradation of phenol and BPA at a pH-NaCl condition similar to those in Group II. The experimental conditions for all seven groups are summarized in Table 1.

Kinetic data were analyzed using first-order kinetic model to describe the apparent rate:

$$\ln\left(\frac{C_t}{C_0}\right) = -kt \tag{1}$$

where C_t and C_o are the SMZ concentrations [mg/L] at time t and time zero, respectively; k is the first order rate constant [min^{-1}]; t is time [min]. In the case where initial SMZ concentration was varied, kinetic data were also analyzed with the Langmuir-Hinshelwood (L-H) model, which is often used to describe surface reactions [24]:

$$r_o = \frac{k_r K C_o}{1 + KC_o} \tag{2a}$$

$$\frac{1}{r_o} = \frac{1}{k_r K}\frac{1}{C_o} + \frac{1}{k_r} \tag{2b}$$

where r_o is the initial rate of reaction [mg/L min]; k_r is the L-H intrinsic rate constant [mg/L min]; K is the L-H adsorption constant [L/mg]; C_o is the aqueous phase initial SMZ concentration [mg/L]. L-H model assumes that adsorption reaction to be rapid and that the rate limiting step is the subsequent transformation of the sorbed species [25].

3. Results and discussion

The surface morphology of the laboratory prepared TiO_2/Ti catalyst is shown in the SEM images (Fig. 1a and b). Fig. 1a shows the aligned nanorod arrays at the surface. Fig. 1b is a cross-sectional view of the nanorod arrays, showing how the nanorods were

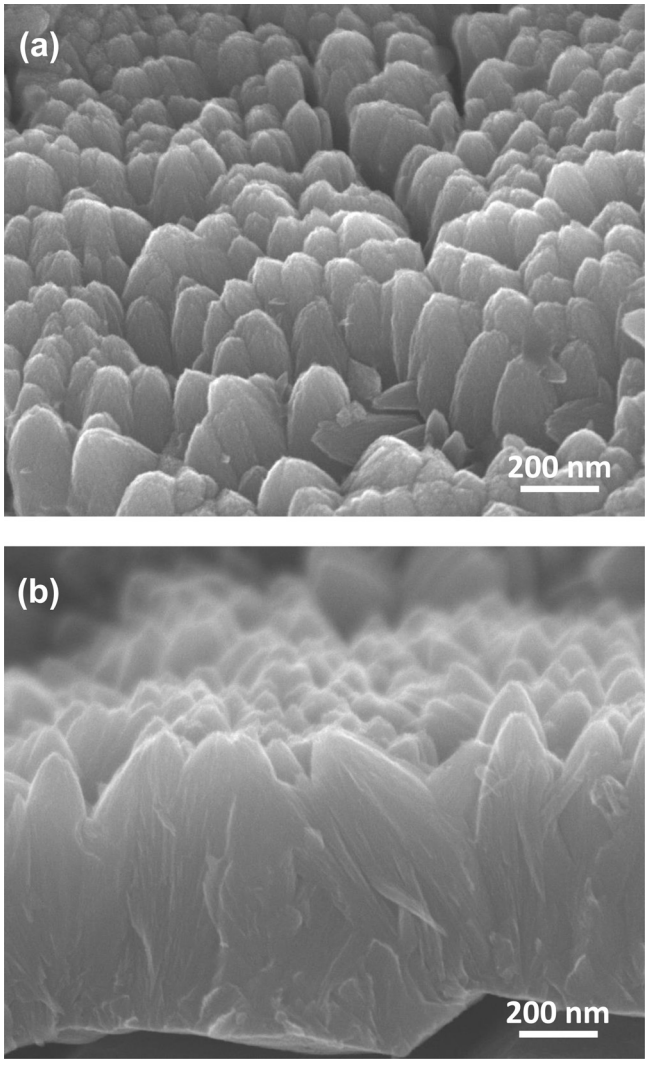

Fig. 1. (a) SEM image of TiO_2 nanorod arrays at the photoanode surface, and (b) cross-sectional view of TiO_2 nanorod arrays.

grown vertical to the Ti foil base. These nanorods were about 100–200 nm in diameter and 800 nm in length. The atomic composition of the nanorods was 32.5% and 67.5% for titanium and oxygen, respectively, suggesting that these crystalline structures were TiO_2. X-ray diffraction analysis (Fig. S1) revealed that the TiO_2 was predominantly rutile. Except the peaks corresponding to the Ti substrate, the diffraction peaks at 27.4° (1 1 0), 36.1° (1 0 1), 41.2° (1 1 1), 54.4° (2 1 1), and 56.7° (2 2 0) can be indexed as the rutile phase of TiO_2. For reference, the often investigated Degussa P25 TiO_2 is approximately 90% anatase and 10% rutile [26] while pure anatase (Hombikat UV-100) and pure rutile TiO_2 (TiOxide) have also been employed in photocatalytic studies [27,28]. The specific surface area of the TiO_2 nanorod array was found to be $2.63 \pm 0.04\ m^2/g$. For reference, the specific surface areas of Degussa P25, Hombikat UV-100, and TiOxide are 50, 186, and $3.5\ m^2/g$, respectively [26–28]. Fig. 2 compares photodegradation of SMZ under photoelectrocatalysis with electrolysis (TiO_2/Ti electrodes in darkness), direct photolysis (UV-A but no TiO_2), and photocatalysis (TiO_2/Ti electrodes + UV-A but no applied potential). No measurable degradation of SMZ was found with electrolysis and direct photolysis. Furthermore, the photocatalytic degradation of SMZ by TiO_2/Ti electrodes under UV-A is slow (about 10% of 2 mg/L SMZ degrades at 90 min). In comparison, SMZ was completely degraded by photoelectrocatalytic reaction after about 70

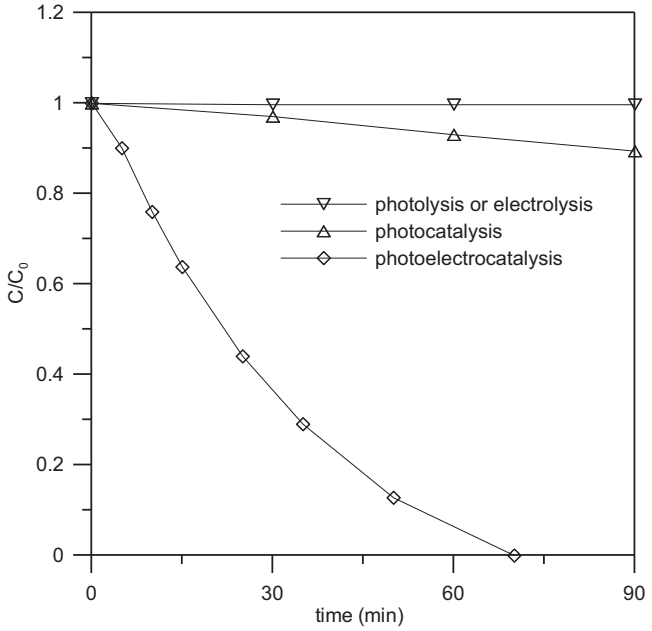

Fig. 2. The degradation of SMZ using photolysis, electrolysis, photocatalysis, and photoelectrocatalysis.

min. The apparent first-order rate constants were $8.3 \times 10^{-4}\ min^{-1}$ and $0.025\ min^{-1}$ for photocatalytic and photoelectrocatalytic reactions, respectively. By applying a biased anodic potential, the photodegradation rate constant of SMZ was increased by 30 times. A comparison on photoelectrocatalytic k with literature values was not made as no photoelectrocatalytic studies on SMZ have been found.

The photocatalytic rate constant obtained here appeared low to those reported in earlier works. Photocatalytic rate constant for antimicrobial agents with TiO_2 as catalyst typically ranged from 0.01 to $0.1\ min^{-1}$: 0.005 to $0.17\ min^{-1}$ [1,10,14] for SMZ, $0.056\ min^{-1}$ for sulfamethazine [29], 0.006–$0.17\ min^{-1}$ for sulfamethizole [30], 0.02–$0.096\ min^{-1}$ for three sulfamate pharmaceuticals [23]. Unlike in this work where laboratory-prepared TiO_2 was used, most of the cited k's were obtained using commercial TiO_2 (i.e., Degussa P25) with direct application or with further modification (e.g., immobilization). P25 TiO_2 is known to have a moderately high specific surface area ($50\ m^2/g$) and is more active in degrading organic contaminants than TiO_2 with other crystalline configurations [1]. The TiO_2 employed in this study, however, had relatively low specific surface area and predominantly rutile phase (Fig. 1c). These two reasons may explain the lower than expected k for SMZ photocatalysis in this study.

Fig. 3 shows the effects of applied anodic potential on the photoelectrocatalytic degradation of SMZ. The results indicate that the degradation rate increased with the applied biased potential. Similar dependence of degradation rate on anodic potential applied was also observed in the photoelectrocatalytic degradation of formic acid [31]. As the anodic potential increased from 0 to 0.5 V vs Ag/AgCl, the rate constant increased from 0.001 to $0.041\ min^{-1}$, and the photocurrent increased from 177 to $348\ \mu A/cm^2$. Since all the applied potential were positive of the flat band potential for TiO_2 in NaCl solution, a potential gradient was established within the TiO_2 film [32]. As the positive potential increased, the resulting gradient separated holes and electrons, decreasing their combination rate, increasing the photocurrent, and accelerating the SMZ degradation rate. Fig. 3b shows that the measured photocurrent increased linearly with the potential applied across the electrodes in agreement with earlier work on photoelectrocatalysis [31].Fig. 4

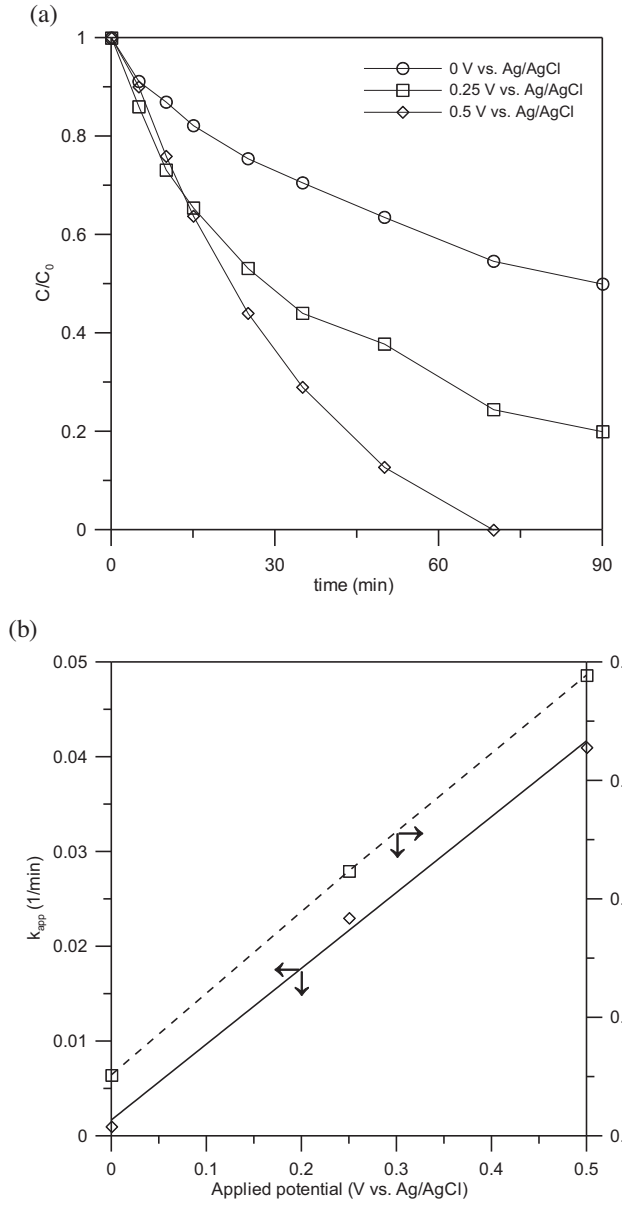

Fig. 3. Effect of applied anodic potential on the photoelectrocatalytic degradation of SMZ.

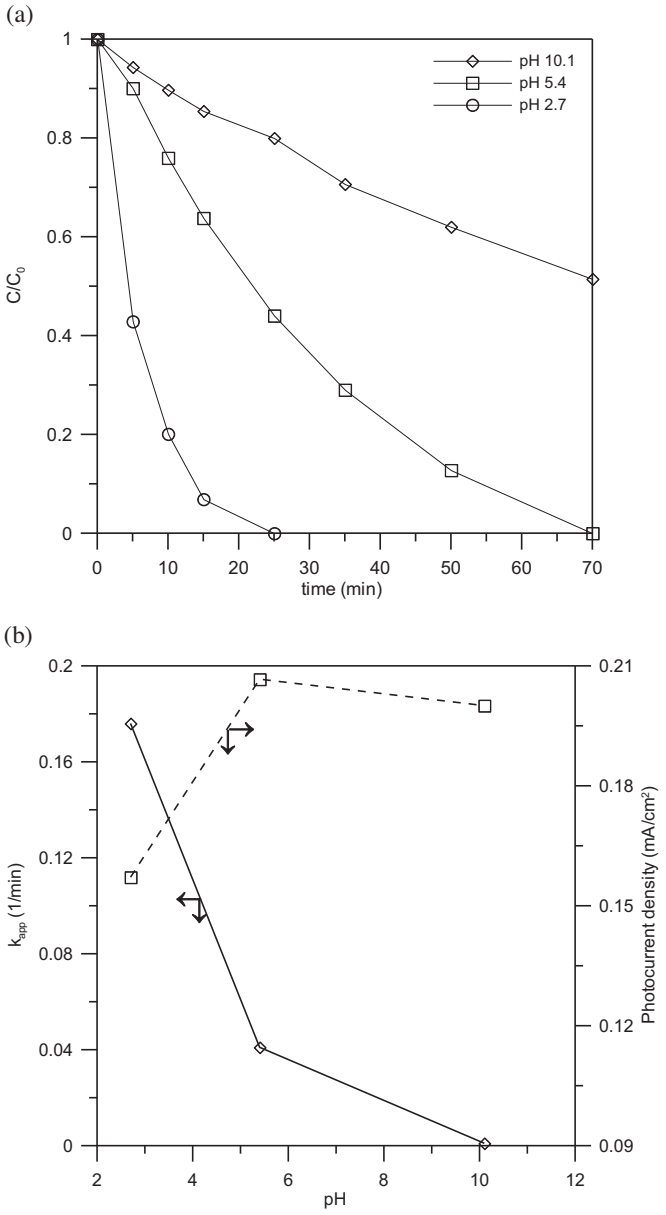

Fig. 4. Effect of solution pH on the photoelectrocatalytic degradation of SMZ.

shows the effects of varying solution pH on the photoelectrocatalytic degradation of SMZ. The degradation rate constant of SMZ decreased from 0.176 to 0.009 min^{-1} with increasing pH from 2.7 to 10.1. The photoelectrocatalytic degradation of SMZ is favored at acidic conditions. However, the photocurrent increased from 0.157 to 0.207 mA/cm^2 with increasing pH from 2.7 to 5.4, and approached a plateau value about 0.200 mA/cm^2 as pH larger than 5.4. The degradation rate increased at acidic pH condition is possibly the result of changes in SMZ acid-base speciation or the extent of SMZ adsorption to TiO_2.

pH is an important system parameter in photoelectrocatalysis as it influences surface charge, agglomeration of catalyst suspension, speciation of organic compounds, and degradation pathway. Since TiO_2 suspension was not used in this study, the effect of pH on agglomeration is irrelevant here. The point of zero charge for TiO_2 is around pH of 6.3–6.7 [1,33], implying that TiO_2 surface will be positively charged at pH 2.7 and 5.4, but negatively charged at pH 10.1 [34]:

$$TiOH + H^+ \leftrightarrow TiOH_2^+ (forpH < pH_{pzc}) \quad (3a)$$

$$TiOH + OH^- \leftrightarrow TiO^- + H_2O (forpH > pH_{pzc}) \quad (3b)$$

SMZ has two acid-base equilibria, with transition from protonated form to neutral form at $pK_{a,1} = 1.85$, and from neutral form to the deprotonated form at $pK_{a,2} = 5.60$ [35]. As a result, the neutral form of SMZ dominates at pH of 2.7, the anionic form prevails at pH of 10.1, while the neutral form and the anionic form are of the same order at pH of 5.4.

The declining rate with pH of 10.1 was consistent with the findings reported in earlier studies [1,36]. Xekoukoulotakis et al. [1] attributed the reduced rate at elevated pH to the reduced adsorption of SMZ due to the repulsion between the negatively charged TiO_2 surface and the deprotonated SMZ at alkaline pH. A more positive surface may further favor the adsorption of SMZ by strengthening the interaction between the positively charged surface and the electron-rich aromatic ring or isoxazole ring. The

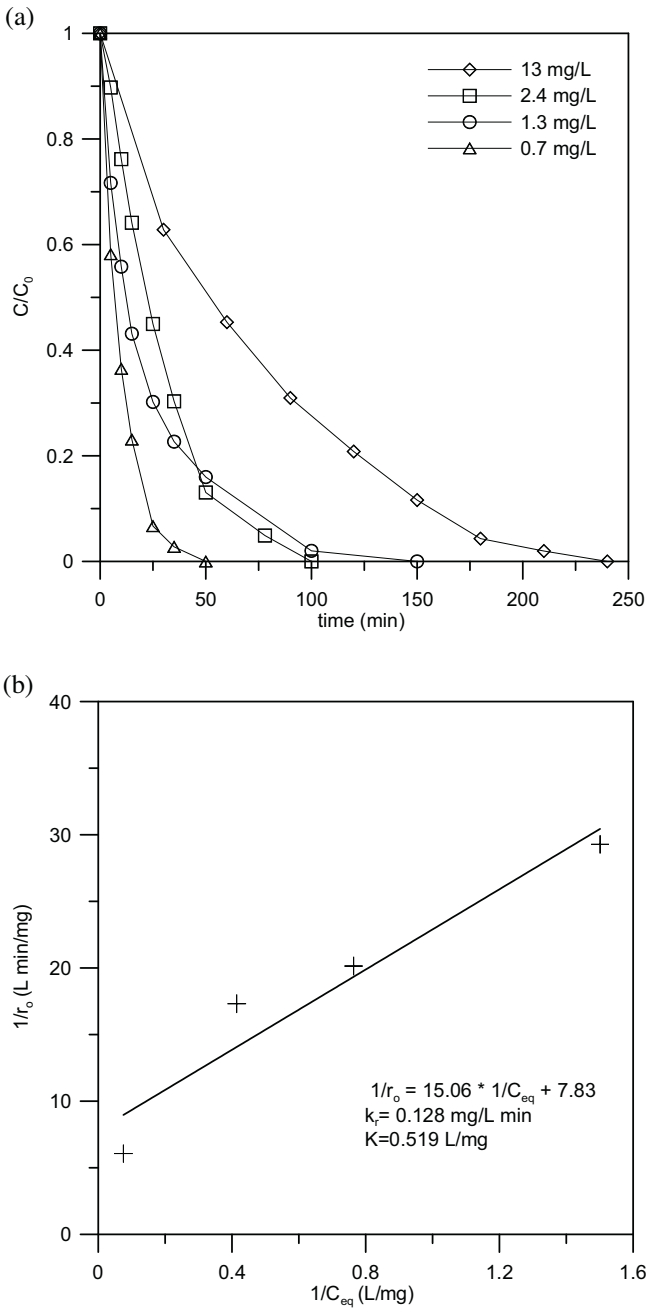

Fig. 5. (a) Effect of initial SMZ concentration on the photoelectrocatalytic degradation of SMZ; (b) the L-H kinetic model for SMZ degradation.

enhanced photodegradation rate at pH 2.7 compared to pH 5.4 may be due to a greater adsorption of SMZ at the TiO_2 surface. Similar reasoning was also used to explain enhanced degradation of quinoline [19] and sulfamated pharmaceuticals [23] at higher pH. Alternatively, the enhanced reactivity at low pH may be explained by the dominant presence of chlorine radicals or active chlorine species over HO• (*see below*).

Fig. 5a shows the influence of the initial SMZ concentration on reaction rates. The relationship between observed rate constant (k_{obs}) and initial SMZ concentration (C_0) is consistent with a Langmuir-Hinshelwood (L-H) kinetic model, often used to describe interfacial reactions [24]. Fig. 5b shows a plot of $1/r_0$ versus $1/C_{eq}$ along with the linear fit of L-H model for the photoelectrocatalytic degradation of SMZ. The fit-derived values for intrinsic reaction rate constant (k_r) and L-H adsorption constant (K) are 0.128 mg/L min and 0.519 L/mg, respectively. Hu et al. [2] and Xekoukoulotakis et al. [1] both investigated photocatalytic degradation of SMZ by UV-A radiation in the presence of P25 TiO_2 suspensions. They reported k_r of 1.7–1.9 mg/L min and K of 0.13–0.17 L/mg. The k_r determined in this work was only 1/10 of the literature values. The lower k_r may be attributed to the different qualities and concentrations of TiO_2 catalyst being used.The K derived from this work was about 3–4 times higher than those reported earlier [1,2]. Adsorption of organic compounds onto TiO_2 may be enhanced by surface modification resulting from UV irradiation or applied anodic potential. By analyzing NMR chemical shift pattern, Yuzawa et al. [37] demonstrated that the electrons of the adsorbed molecules were withdrawn by TiO_2. In the absence of UV irradiation (i.e., dark), adsorption of organic compound onto TiO_2 surface was found to be negligible [1]. The application of UV irradiation will lead to the generation of electron-hole pairs, where the holes, h^+_{VB}, will favor the electron withdrawal by TiO_2 surface, thereby promoting adsorption. When a bias potential is applied on top of UV irradiation, the potential will discourage the recombination of electron-hole pairs, and thus further facilitates the adsorption of organic compounds on TiO_2 surface.

Fig. 6 shows the effect of NaCl electrolyte concentration on degradation of SMZ by TiO_2/Ti. The degradation rate constant of SMZ increased from 0.01 to 0.14 min^{-1} with increasing NaCl concentration from 1 to 100 mM. The results show that the addition of NaCl was an effective way to improve the photoelectrocatalytic degradation of SMZ. On the other hand, the photocurrent increased from 0.074 to 0.140 mA/cm^2 with increasing NaCl concentrtion from 1 to 10 mM. Further increase in NaCl level beyond 10 mM had no influence on photocurrent, although k was further improved to 0.14 min^{-1}.

In the presence of chloride, photoelectrocatalytic degradation of SMZ may proceed through the formation of the chlorine radicals and active chlorine species ($HOCl/Cl_2$) in addition to HO•. Yuan et al. [38] proposed that chlorine radicals and active chlorine species contributed to the degradation of dye compound in a cobalt-peroxymonosulfate oxidation system, with the detection of chlorinated aromatic intermediates as evidence. Zanoni et al. [39] reported the production of active chlorine via photoelectrocatalysis of Cl^- with TiO_2 electrode though without suggesting a clear formation mechanism linking chlorine formation to HO•. $HOCl/Cl_2$ are strong oxidants and are capable of trapping the photo-generated electrons [40].

The following mechanism is presented to account for the production of chlorine radicals, active chlorine species, and related pH-dependent speciation reactions following the works by Yu et al. [41] Yuan et al [38] Zanoni et al [39] and known chlorine chemistry [42]:

$$HO^\bullet + Cl^- \leftrightarrow ClOH^{\bullet -} \quad (4a)$$

$$ClOH^{\bullet -} + H^+ \leftrightarrow Cl^\bullet + H_2O \quad (4b)$$

$$Cl^\bullet + Cl^- \leftrightarrow Cl^\bullet_2{}^- \quad (4c)$$

$$Cl^\bullet_2{}^- + H_2O \rightarrow ClOH^{\bullet -} + H^+ + Cl^- \quad (4d)$$

$$Cl^\bullet_2{}^- + Cl^\bullet_2{}^- \rightarrow Cl_2 + 2Cl^- \quad (5a)$$

$$Cl^\bullet_2{}^- + Cl^\bullet \rightarrow Cl_2 + Cl^- \quad (5b)$$

$$Cl_2 + H_2O \leftrightarrow HOCl + H^+ + Cl^- \quad (6a)$$

$$HOCl \leftrightarrow H^+ + OCl^- \quad (6b)$$

with $K_{4a} = 0.70\ (\pm 0.13)\ M^{-1}$, $K_{4b} = 7.2\ (\pm 1.6) \times 10^6$ (water excluded in K_{4b}), $K_{4c} = 1.4\ (\pm 0.13) \times 10^5\ M^{-1}$ [41]; $K_{6a} = 4.5 \times 10^{-4}\ M^2$ (water already incorporated in K_{6a}); $K_{6b} = 3 \times 10^{-8}\ M$ [42]. The consequence of the listed reactions are the production and propagation of reactive chlorine species (RCS) (i.e. $ClOH^{\bullet -}$, $Cl^\bullet$, $Cl^\bullet_2{}^-$) (Eqs. (4a)

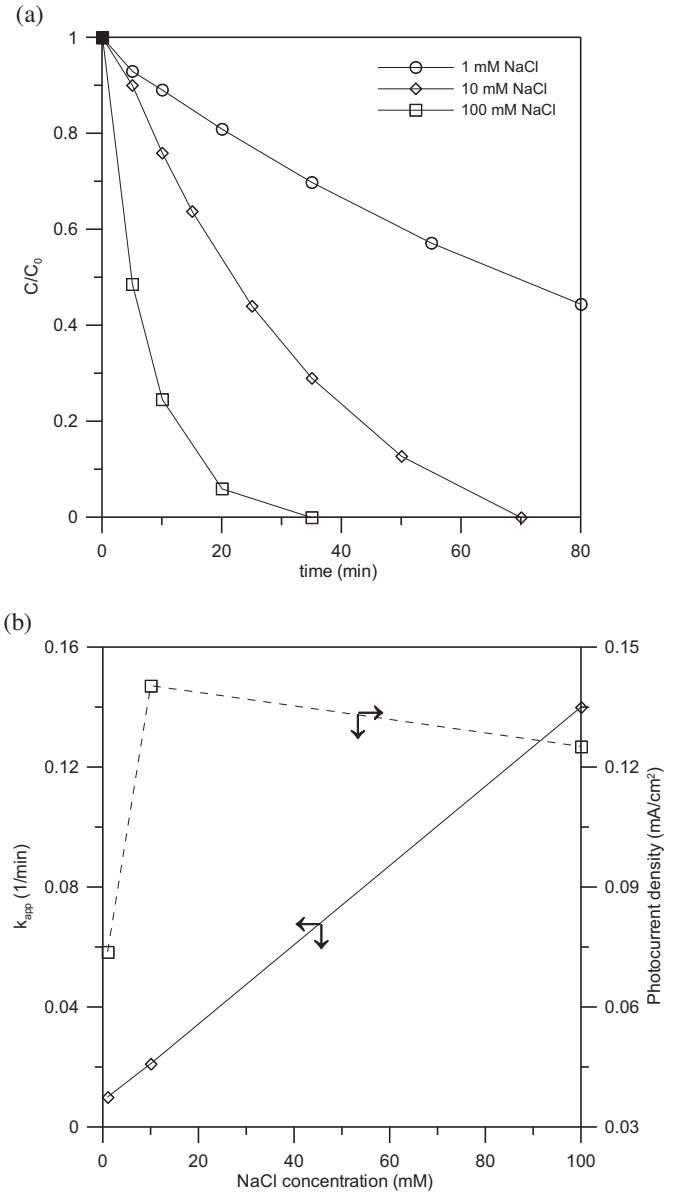

Fig. 6. Effect of NaCl concentration on the photoelectrocatalytic degradation of SMZ.

to (4d)) and the production of active chlorine (Cl_2) following the termination of the chlorine radicals chain reaction (Eqs. (5a) and (5b)).

The concentrations of reactive oxidizing species may be estimated with assumptions. It was assumed that the reaction rate depends on both the concentrations of SMZ and HO• with the concentrations of HO• remains constant as long as TiO_2 is illuminated. So that the following may be expressed:

$$-r_o = k_{HO\bullet} C_{HO\bullet} C_{SMZ} = kC_{SMZ} \quad (7a)$$

where k is the apparent first order rate constant observed in this experiment [s^{-1}]; C_{SMZ} is the SMZ concentration [M]; $k_{HO\bullet}$ is the second-order rate constant for hydroxyl-SMZ reaction [$M^{-1}s^{-1}$]; $C_{HO\bullet}$ is the concentration of hydroxyl radicals [M]. $k_{HO\bullet}$ between HO• and most aromatic compounds ranged between 10^9–10^{10} $M^{-1}s^{-1}$ [43], with 10^{10} $M^{-1}s^{-1}$ being the limit for diffusion-controlled reactions [44]. Using a k of 9.86×10^{-4} min^{-1} (or 1.64×10^{-5} s^{-1}) for no NaCl case and taking a geometric mean of 3.2×10^9 $M^{-1}s^{-1}$ for $k_{HO\bullet}$, $C_{HO\bullet}$ was estimated to be 5.1×10^{-15} M. Liao and Reitberger [33] reported a HO• generation rate of approximately 2 μM/min (or 3.3×10^{-8} M/s) across pH of 3–11 in a UV-A illuminated TiO_2 system. Taking the simple assumption that the rate of HO• is proportional to the illuminated area, the reported HO• rate will translate into 1.7×10^{-10} M/s for this study (TiO_2 surface in this study ~ 1/200 of that in Liao and Reitberger [33]). Further assuming production rate and consumption rate of HO• is balanced so that a steady state $C_{HO\bullet}$ can be determined as:

$$r_{production} = -r_{consumption} = k_{HO\bullet} C_{HO\bullet} C_{SMZ} \quad (7b)$$

With $r_{production} = 1.7 \times 10^{-10}$ M/s, $k_{HO\bullet} = 3.2 \times 10^9 M^{-1}s^{-1}$, and $C_{SMZ} = 9.5 \times 10^{-6} M$, $C_{HO\bullet}$ was estimated to be 5.6×10^{-15} M, which was quite close to 5.1×10^{-15} M as estimated by Eq. (7a).

Analysis on the molar ratios of HO• and chlorine-based radicals further supports that elevated chloride level can give rise to RCS or active chlorine that enhances photodegradation of SMZ. Using the equilibrium constants provided by Yu et al. [41] (i.e., K_{4a}, K_{4b}, and K_{4c}), the ratios between HO• and each of the three major RCS (i.e., $ClOH^{\bullet -}$, $Cl^\bullet$, $Cl^\bullet_2^-$) can be determined at any given pH and Cl^- level:

$$\frac{[ClOH^{\bullet -}]}{[HO^\bullet]} = \frac{[Cl^-]}{1.43} \quad (8a)$$

$$\frac{[Cl^\bullet]}{[HO^\bullet]} = \frac{[Cl^-][H^+]}{1.1 \times 10^{-5}} \quad (8b)$$

$$\frac{[Cl^\bullet_2^-]}{[HO^\bullet]} = \frac{[Cl^-]^2[H^+]}{8.0 \times 10^{-11}} \quad (8c)$$

where [*species*] denotes molar concentration [M].

The reactivity of RCS (i.e., $ClOH^{\bullet -}$, $Cl^\bullet$, $Cl^\bullet_2^-$) towards SMZ, phenol, and BPA, measurable by the respective second order rate constants, is expected to be within a 10–100 of those associated with HO•. All three examined chemicals were aromatic compounds with electron donating substituents (i.e., —OH, lone pair e^-). Flash photolysis data [45] suggested that the second-order $k_{Cl^\bullet_2^-}$'s towards aromatic chemicals with e^- donating substituents, such as SMZ, phenol, and BPA, typically ranges from 10^8 to 10^9 M^{-1} s^{-1}. For $Cl^\bullet$, $k_{Cl^\bullet} > k_{Cl^\bullet_2^-}$ is expected as chlorine atom is more reactive than $Cl^\bullet_2^-$ [46,47]. With HO• as the oxidant, $k_{HO\bullet}$ between 10^8 to 10^{10} $M^{-1}s^{-1}$ is expected [44,48]. This implies that RCS can surpass HO• as the main oxidant when their presence is favored by system factors such as chloride ion concentration or pH.

Since the reactivity of RCS and active chlorine is unlikely to exceed HO• [44,48] to show that RCS or active chlorine may be important, one need to demonstrate their concentrations are at least comparable to, if not exceeding, that of HO• in the system. For illustration, the molar ratios of radicals listed in Eq. (8a)–(8c) and the experimental k for four pH-NaCl conditions are summarized (Table 2). The four cases were selected to represent two slow ($k = 0.01$ min^{-1}) and two fast ($k \geq 0.1$ min^{-1}) cases with varying pH and Cl^- levels. From Table 2, it can be seen that $ClOH^{\bullet -}$ is considered as a minor species to HO• in all four cases (i.e., $[ClOH^{\bullet -}]/[HO^\bullet] \ll 1$) and $Cl^\bullet$ may be comparable with HO• occasionally. The important RCS appears to be $Cl_2^{\bullet -}$ as its dominance coincides with the magnitude of k: $[Cl_2^{\bullet -}] \gg [HO^\bullet]$ when k is fast (i.e., 0.14–0.18 min^{-1}) but $[Cl_2^{\bullet -}] \ll [HO^\bullet]$ when k is slow. $Cl_2^{\bullet -}$ may react directly with SMZ or form Cl_2 via Equation 5a and 5b. The production rate of Cl_2 can be estimated by considering the forward rates of Equation 5a and 5b involving $Cl_2^{\bullet -}$ and $Cl^\bullet$:

$$r_{Cl_2} = k_{5a} C^2_{C^\bullet_{l_2^-}} + k_{5b} C_{Cl^\bullet_2^-} C_{Cl^\bullet} \quad (9)$$

where $k_{5a} = 9 \times 10^8$ $M^{-1}s^{-1}$ and $k_{5b} = 2.1 \times 10^9$ $M^{-1}s^{-1}$ [41]. Following Equation 8b and 8c and the $[HO^\bullet]_{ss}$ estimate of ~ 5×10^{-15} M, it can be shown that $r_{Cl2} = 10^{-15}$ to 10^{-13} M/s for the high k cases (Table 2) but only 10^{-28} to 10^{-23} M/s for the slow k cases. This

Table 2
Molar ratios of reactive chlorine species to hydroxyl radical at selected pH and NaCl levels.

pH	C_{NaCl} (mM)	k (min^{-1})	$\frac{[ClOH^{\bullet-}]}{[HO]^{\bullet}}$	$\frac{[Cl^{\bullet}]}{[HO^{\bullet}]}$	$\frac{\left[Cl_2^{\bullet-}\right]}{[HO^{\bullet}]}$	$t_{[Cl_2]_{tot}\rightarrow[HO^{\bullet}]}$
5.7	1	0.01	7×10^{-4}	3.6×10^{-4}	0.05	9×10^{7} s
10.1	10	0.01	0.007	7.1×10^{-8}	1.0×10^{-4}	2×10^{13} s
2.7	10	0.18	0.007	1.8	2500	0.04 s
5.7	100	0.14	0.07	0.036	500	0.9 s

means that the total active chlorine can build up to the same level as $[HO^{\bullet}]_{ss}$ in less than 1 s for the fast k cases, but at least 1000+ h in the slow k cases ($t_{[Cl_2]_{tot}\rightarrow[HO^{\bullet}]}$ in Table 2). This analysis demonstrates the critical role of Cl^- ion in contributing the reactive $Cl_2^{\bullet-}$ or active chlorine species in quantity or rate that is significant to the overall rate of SMZ photodegradation. Consequently, higher NaCl concentration could enhance the photoelectrocatalytic degradation of SMZ.

A consistent understanding on the role of Cl^- and other inorganic ions in advanced oxidation system is still lacking due to apparently conflicting results gathered from different studies. In this work, degradation rate was found to increase with higher NaCl concentration. An et al. [19] also reported Cl^--enhanced quinoline photodegradation up to as high as 1 M NaCl. Abdullah et al. [49], however, found that photodegradation rate declined with increasing Cl^- concentration for salicyclic acid, aniline, and ethanol over 0–100 mM NaCl. Similarly, Grebel et al [50] reported that the degradation rate of phenol in a UV/H_2O_2 system declined with increasing concentration of Br^-, Cl^-, and carbonate ions. In contrast, Yuan et al. [38] investigated the degradation of an azo dye in a catalytic Co-peroxymonosulfate catalytic over 0–500 mM of NaCl and found that the degradation rate was highest at 0 and 500 mM NaCl, with the lowest rate observed at 5 mM NaCl. Carneiro et al. [36] also studied the degradation of an azo dye, and found that degradation rate was favored at pH <6 if NaCl was used but at pH >10 if Na_2SO_4 was employed, suggesting that pH and inorganic ion effects are likely coupled. Grebel et al. [50], however, observed that the degradation rate of cyclohexanol always declined with increasing Br^- or Cl^- concentrations for pH between 3 to 9. While individual explanations or hypotheses have been offered (e.g., reduced $HO^{\bullet}$ production due to inorganic ions competing for surface holes [49], or that reactive halogen radicals react more selectively with compounds having electron-rich fragments [50]), no proposed theory has been successful in reconciling the different experimental observations reported so far.

Fig. 7 shows the influence of humic acid and methanol on SMZ degradation. The presence of 10 mg/L humic acid had measurable effect on SMZ degradation, while 10% methanol significantly reduced the reaction. The degradation rate constants were 0.013 and 0.001 min^{-1} in the presence of 10 mg/L humic acid and 10% methanol, respectively, while the rate constant was 0.021 min^{-1} for the baseline case without radical scavenger (SMZ only). In contrast, the photocurrents were 0.144 and 0.461 mA/cm^2 in the presence of 10 mg/L humic acid and 10% methanol, respectively, while the photocurrent was 0.140 mA/cm^2 for SMZ alone. The destruction of humic acid and alcohol in TiO_2-photoelectrocatalytic system have been reported in the past [49]. Humic acid and methanol are known scavengers of hydroxyl radicals [51,52], and hence inhibitory effect on photoelectrocatalytic degradation of SMZ was expected with their presence.

The photocurrent measured for the 10% methanol experiment (0.461 mA/cm^2) was substantially higher than the typical range of ≤0.200 μA/cm^2 observed in this study. The exceptional high photocurrent seems to suggest that *current doubling* was happening in the presence of methanol. *Current doubling* refers to the release of additional electron from the formation of a reactive solute-hole intermediate that results in additional electron production and flow [53,54]. Since one electron is released when photon is absorbed by the surface and a second electron is released from the solute-hole intermediate, a maximum of two electrons flow per photon absorbed may be expected [54]. It is hypothesized that methanol may form the solute-hole intermediate upon the formation of the valence-band hole, producing a methoxy radical ($CH_3O^{\bullet}$) and a H^+

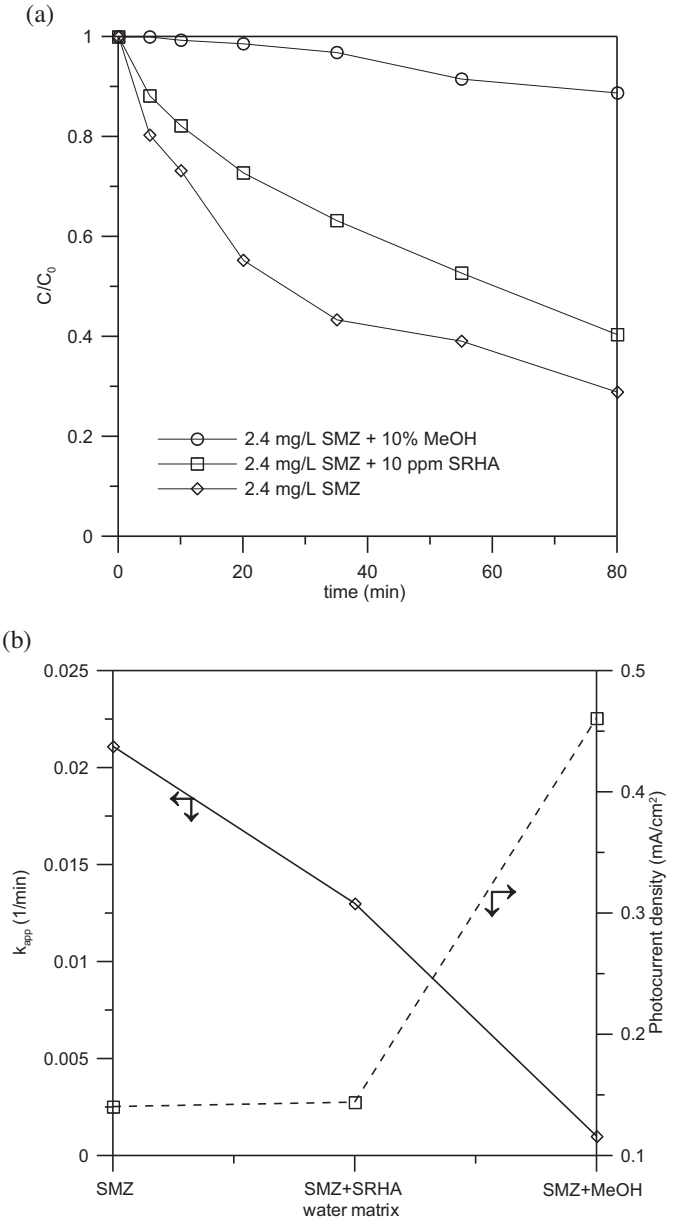

Fig. 7. Effect of water matrix (humic acid and methanol) on the photoelectrocatalytic degradation of SMZ.

(Eq. (10a)). The methoxy radical is then oxidized to formaldehyde and release the second H^+ and electron (Eq. (10b)) simultaneously:

$$CH_3OH + h^+_{VB} \rightarrow CH_3O^\bullet + H^+ \quad (10a)$$

$$CH_3O^\bullet \rightarrow CH_2O + H^+ + e^-_{CB} \quad (10b)$$

where h^+_{VB} refers to the valance-band hole formed upon the absorption of photon, and e^-_{CB} refers to the electron released into the conductance band. The resulting formaldehyde is rapidly hydrated to form methanediol ($H_2C(OH)_2$; Eq. (11a)), which can further react with $HO^\bullet$ (Eq. (11b)) and eventually generate formic acid as the major reaction product (Eq. (11c)) [55]:

$$HCHO + H_2O \leftrightarrow H_2C(OH)_2 \quad (11a)$$

$$HO^\bullet + H_2C(OH)_2 \rightarrow HC(OH^\bullet)_2 + H_2O \quad (11b)$$

$$HC(OH^\bullet)_2 + O_2 \rightarrow HO^\bullet_2 + HCOOH \quad (11c)$$

The formic acid would then further initiate another current doubling reaction [31] in similar manner as Equation 10a and 10b:

$$HCOOH + h^+_{VB} \rightarrow HCOO^\bullet + H^+ \quad (12a)$$

$$HCOO^\bullet \rightarrow CO_2 + H^+ + e^-_{CB} \quad (12b)$$

The coupling of two sequential current doubling reaction can explain why the photocurrent in 10% methanol (0.461 mA/cm^2) was more than three times that observed with humic acid (0.144 mA/cm^2) or with the SMZ control (0.140 mA/cm^2).

Photocurrent may be used as an indirect measure of the effectiveness of charge separation for it quantifies the flow of electrons driven to the counter electrons under an applied anodic bias potential. It is often expected that the rate of photodegradation will increases with better charge separation (Fig. 2b [56]). Results from this study demonstrated that a higher photocurrent does not necessarily lead to an improved photodegradation rate. This has been demonstrated in Figs. 4b, 6b, and 7b which collectively illustrated that the photoelectrocatalytic efficiency can be influenced by system pH, ionic strength, and the presence of radical scavengers. In the context of wastewater treatment operation, this implies that further control on the process rate is available through manipulation on the chemical environment in addition to the voltage applied.

Fig. 8 shows the photoelectrocatalytic degradation of phenol and BPA at pH of 5.4, 10 mM NaCl, and 0.5 V. Negligible loss of phenol and BPA was observed in the control experiments, where both irradiation and anodic potential were not applied. The first order rate constant, k, for phenol and BPA were 0.006 and 0.010 min^{-1}, respectively. 30% and 45% of the initial phenol and BPA, respectively, were photodegraded within 60 min. For phenol, <5 to 65% photodegradation have been reported for various photocatalytic TiO_2 systems [57,58], with as high as 90% conversion reported with Degussa P-25 TiO_2 [59]. The 30% conversion observed here fell within the typical range reported. For BPA, Kang et al. [60]; reported a 20% conversion within an hour in a Fe-TiO_2 photocatalytic system while Luo et al. [61] reported a 10–40% conversion over various fluorinated anatase TiO_2 photocatalysts, suggesting a better BPA conversion with our photoanode. The conversion of both compounds can be further improved by fine tuning operational parameters such as pH, NaCl, and anodic potential.

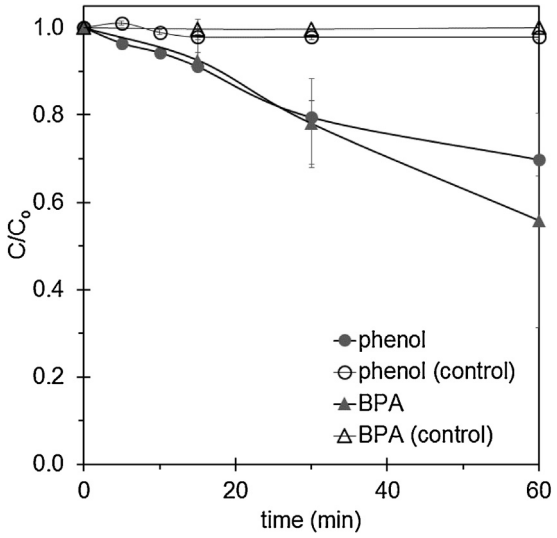

Fig. 8. Photoelectrocatalytic degradation of phenol (2.4 mg/L) and bisphenol-A (2.4 mg/L) at pH of 5.4, 10 mM NaCl, and an anodic potential of 0.5 V. No UV-A irradiation in the control experiments.

4. Conclusions

This study demonstrated that TiO_2/Ti-photoelectrocatalysis is an effective method for the degradation of SMZ in aqueous solutions. Under PEC, complete degradation of SMZ was observed within 70 min with a rate that was approximately 30 times that of photocatalysis. Langmuir-Hinshelwood analysis on the degradation kinetic data of SMZ revealed that photoadsorption may be enhanced in the presence of applied anodic potential, with K being 3–4 times of those from photocatalysis.

Process performance was affected by applied anodic potential, solution pH, NaCl concentrations, and the presence of radical scavengers. SMZ degradation was enhanced with higher applied anodic potential and NaCl concentration and lower solution pH and concentration radical scavengers. Further analysis suggested that the high level of PEC activity was observed when [$Cl_2^{\bullet-}$] dominated over [$HO^\bullet$]. The inhibitory effect of radical scanvegers on SMZ degradation also confirmed the importance of radicals in SMZ photoelectrocatalysis. The introduction of methanol caused photocurrent to increase by 3 times above the average. This may be explained by sequential current doubling through the conversion of h^+_{VB}-bound to formaldehyde, oxidation of formaldehyde by $HO^\bullet$ to formic acid, and oxidation of h^+_{VB}-bound formic acid to CO_2.

This work suggested that the enhanced photodegradation of SMZ may be related to the higher level of photoadsorption of the compound to TiO_2 catalyst surface. It is unclear how photoadsorption of sorbate is influenced by the anodic bias potential applied. It may be worthwhile to investigate the dependence of K, the L-H adsorption constant, at various voltage over a defined concentration ranges of SMZ and other pharmaceuticals. Similarly, dependence of K on pH for SMZ and other pH-sensitive antimicrobial compounds would allow a better understanding on how surface charge and compound chemical structure affect adsorption.

It would also be beneficial to conduct similar photoelectrocatalytic experiments on several benchmark pharmaceuticals over TiO_2 suspensions [1] and other commonly employed immobilized TiO_2 systems [10] so that the kinetic performance of photoelectrocatalysis can be properly referenced to photocatalysis.

Molar analysis of $HO^\bullet$ and chlorine radicals and the observed k at different pH-[Cl^-] conditions clearly demonstrated the importance of considering pH, anion type and concentration together (Table 2). With $Cl_2^{\bullet-}$ dominating over $HO^\bullet$ in all the noticeable instances in this study, the results also hinted that $HO^\bullet$, despite its superior reactivity and oxidizing power, may not be the main driver of organic contaminant oxidation in photoelectrocatalysis. Further understanding on the role of chlorine radicals and active chlorine species in the degradation of organic contaminants will

help define a critical set of chemical parameters needed for practical PEC application.

Acknowledgments

The authors gratefully acknowledge the financial support of the National Science Council of Taiwan, R. O. C. DK was supported by National Natural Science Foundation of China (Project No. 21477100) and Strategic Research Grant (Grant No. 7004184).

Appendix A. Supplementary data

Supplementary data associated with this article can be found, in the online version, at http://dx.doi.org/10.1016/j.apcatb.2016.01.003.

References

[1] N.P. Xekoukoulotakis, C. Drosou, C. Brebou, E. Chatzisymeon, E. Hapeshi, D. Fatta-Kassinos, D. Mantzavinos, Catal. Today 161 (2011) 163–168.
[2] L.H. Hu, P.M. Flanders, P.L. Miller, T.J. Strathmann, Water Res. 41 (2007) 2612–2626.
[3] W. Baran, E. Adamek, A. Sobczak, A. Makowski, Appl. Catal. B—Environ. 90 (2009) 516–525.
[4] K. Kummerer, Chemosphere 75 (2009) 417–434.
[5] S. Kaneco, H. Katsumata, T. Suzuki, K. Ohta, Chem. Eng. J. 125 (2006) 59–66.
[6] R. Andreozzi, L. Campanella, B. Fraysse, J. Garric, A. Gonnella, R. Lo Giudice, R. Marotta, G. Pinto, A. Pollio, Water Sci. Technol. 50 (2004) 23–28.
[7] W. Baran, J. Sochacka, W. Wardas, Chemosphere 65 (2006) 1295–1299.
[8] F.J. Beltran, A. Aguinaco, J.F. Garcia-Araya, A.L. Oropesa, Water Res. 42 (2008) 3799–3808.
[9] N. Klamerth, N. Miranda, S. Malato, A. Aguera, A.R. Fernandez-Alba, M.I. Maldonado, J.M. Coronado, Catal. Today 144 (2009) 124–130.
[10] N. Miranda-Garcia, S. Suarez, B. Sanchez, J.M. Coronado, S. Malato, M.I. Maldonado, Appl. Catal. B—Environ. 103 (2011) 294–301.
[11] D. Nasuhoglu, V. Yargeau, D. Berk, J. Hazard. Mater. 186 (2011) 67–75.
[12] F.J. Rivas, F.J. Beltran, A. Encinas, J. Environ. Manage. 100 (2012) 10–15.
[13] M.N. Abellan, B. Bayarri, J. Gimenez, J. Costa, Appl. Catal. B—Environ. 74 (2007) 233–241.
[14] M.N. Abellan, J. Gimenez, S. Esplugas, Catal. Today 144 (2009) 131–136.
[15] B. Bayarri, M.N. Abellan, J. Gimenez, S. Esplugas, Catal. Today 129 (2007) 231–239.
[16] L. Xu, G. Wang, F.Y. Ma, Y.H. Zhao, N. Lu, Y.H. Guo, X. Yang, Appl. Surf. Sci. 258 (2012) 7039–7046.
[17] E.R.A. Ferraz, G.A.R. Oliveira, M.D. Grando, T.M. Lizier, M.V.B. Zanoni, D.P. Oliveira, J. Environ. Manage. 124 (2013) 108–114.
[18] T. An, G. Li, X. Zhu, J. Fu, G. Sheng, Z. Kun, Appl. Cata. A: Gen. 279 (2005) 247–256.
[19] T. An, W. Zhang, X. Xiao, G. Sheng, J. Fu, X. Zhu, J. Photochem. Photobiol. A: Chem. 161 (2004) 233–242.
[20] G. Li, X. Liu, T. An, H. Yang, S. Zhang, H. Zhao, Catal. Today 242 (2015) 363–371.
[21] G. Li, T. An, J. Chen, G. Sheng, J. Fu, F. Chen, S. Zhang, H. Zhao, J. Hazard. Mater. 138 (2006) 392–400.
[22] X. Nie, J. Chen, G. Li, H. Shi, H. Zhao, P.-K. Wong, T. An, J. Chem. Technol. Biotechnol. 88 (2013) 1488–1497.
[23] H. Yang, G. Li, T. An, Y. Gao, J. Fu, Catal. Today 153 (2010) 200–207.
[24] M.R. Hoffmann, S.T. Martin, W.Y. Choi, D.W. Bahnemann, Chem. Rev. 95 (1995) 69–96.
[25] P.L. Houston, Chemical Kinetics and Reaction Dynamics, 1st ed., McGraw-Hill, Dubuque, Iowa, 2001.
[26] G.V. Nano, T.J. Strathmann, J. Colloid Interface Sci. 297 (2006) 443–454.
[27] H. Tahiri, N. Serpone, R. Le Van Mao, J. Photochem. Photobiol. A: Chem. 93 (1996) 199–203.
[28] D. Vasudevan, A.T. Stone, J. Colloid Interface Sci. 202 (1998) 1–19.
[29] S. Kaniou, K. Pitarakis, I. Barlagianni, I. Poulios, Chemosphere 60 (2005) 372–380.
[30] D. Klauson, M. Krichevskaya, M. Borissova, S. Preis, Environ. Technol. 31 (2010) 1547–1555.
[31] R.J. Candal, W.A. Zeltner, M.A. Anderson, Environ. Sci. Technol. 34 (2000) 3443–3451.
[32] K. Vinodgopal, S. Hotchandani, P.V. Kamat, J. Phys. Chem. 97 (1993) 9040–9044.
[33] H.D. Liao, T. Reitberger, Catalysts 3 (2013) 418–443.
[34] Y.Z. Zhang, X.Y. Xiong, Y. Han, X.H. Zhang, F. Shen, S.H. Deng, H. Xiao, X.Y. Yang, G. Yang, H. Peng, Chemosphere 88 (2012) 145–154.
[35] Z.M. Qiang, C. Adams, Water Res. 38 (2004) 2874–2890.
[36] P.A. Carneiro, M.E. Osugi, J.J. Sene, M.A. Anderson, M.V.B. Zanoni, Electrochim. Acta 49 (2004) 3807–3820.
[37] H. Yuzawa, M. Aoki, H. Itoh, H. Yoshida, J. Phys. Chem. Lett. 2 (2011) 1868–1873.
[38] R.X. Yuan, S.N. Ramjaun, Z.H. Wang, J.S. Liu, J. Hazard. Mater. 196 (2011) 173–179.
[39] M.V.B. Zanoni, J.J. Sene, H. Selcuk, M.A. Anderson, Environ. Sci. Technol. 38 (2004) 3203–3208.
[40] E. Pelizzetti, V. Carlin, C. Minero, M. Gratzel, New J. Chem. 15 (1991) 351–359.
[41] X.Y. Yu, Z.C. Bao, J.R. Barker, J. Phys. Chem. A 108 (2004) 295–308.
[42] G. Tchobanoglous, F.L. Burton, H.D. Stensel, Metcalf, Eddy, Wastewater Engineering: Treatment and Reuse, McGraw-Hill Education, 2003, 2016.
[43] W.R. Haag, C.C.D. Yao, Environ. Sci. Technol. 26 (1992) 1005–1013.
[44] P.M. Schwarzenbach, Environmental Organic Chemistry, 2nd ed., Wiley Hoboken, N.J, 2003.
[45] K. Hasegawa, P. Neta, J. Phys. Chem. 82 (1978) 854–857.
[46] B.C. Gilbert, J.K. Stell, W.J. Peet, K.J. Radford, J. Chem. Soc. Faraday Trans. 1 84 (1988) 3319–3330.
[47] M.L. Alegre, M. Geronés, J.A. Rosso, S.G. Bertolotti, A.M. Braun, D.O. Mártire, M.C. Gonzalez, J. Phys. Chem. A 104 (2000) 3117–3125.
[48] Y. Lee, U. von Gunten, Water Res. 44 (2010) 555–566.
[49] M. Abdullah, G.K.C. Low, R.W. Matthews, J. Phys. Chem. 94 (1990) 6820–6825.
[50] J.E. Grebel, J.J. Pignatello, W.A. Mitch, Environ. Sci. Technol. 44 (2010) 6822–6828.
[51] S. Nelieu, L. Kerhoas, J. Einhorn, Int. J. Environ. Anal. Chem. 65 (1996) 297–311.
[52] X.J. Yan, R.L. Bao, S.L. Yu, Q.F. Li, Q.F. Jing, Russ. J. Phys. Chem. A 86 (2012) 1479–1485.
[53] S.R. Morrison, T. Freund, J. Chem. Phys. 47 (1967), 1543-&.
[54] Y. Maeda, A. Fujishima, K. Honda, J. Electrochem. Soc. 128 (1981) 1731–1734.
[55] W.J. McElroy, S.J. Waygood, J. Chem. Soc., Faraday Trans. 87 (1991) 1513–1521.
[56] G.G. Bessegato, T.T. Guaraldo, M.V.B. Zanoni, Enhancement of Photoelectrocatalysis Efficiency by Using Nanostructured Electrodes, InTech Open, 2014.
[57] H. Ling, K. Kim, Z. Liu, J. Shi, X. Zhu, J. Huang, Catal. Today 258 (2015) 96–102.
[58] M.E. Borges, M.C. Alvarez-Galván, P. Esparza, E. Medina, P. Martín-Zarza, J.L.G. Fierro, Energy Environ. Sci. 1 (2008) 364.
[59] S.-J. Tsai, S. Cheng, Catal. Today 33 (1997) 227–237.
[60] S. Kang, J.Y. Do, S.W. Jo, K.M. Kim, K.M. Jeong, S.-M. Park, M. Kang, Bull. Korean Chem. Soc. 36 (2015) 2006–2014.
[61] L. Luo, Y. Yang, A. Zhang, M. Wang, Y. Liu, L. Bian, F. Jiang, X. Pan, Appl. Surf. Sci. 353 (2015) 469–479.